

# **STRAIN FIELD OF REINFORCED CONCRETE UNDER ACCELERATED CORROSION BY DIGITAL IMAGE CORRELATION TECHNIQUE**

Zuquan Jin<sup>1</sup>, Yun Bai<sup>2</sup>, Tiejun Zhao<sup>1</sup>, Yudan Jiang<sup>1</sup>, Yongfeng Chen<sup>1</sup>

<sup>1</sup> College of Civil Engineering, Qingdao Technological University, Qingdao, China

<sup>2</sup>Advanced and Innovative Materials (AIM) Group, Department of Civil, Environmental & Geomatic engineering, University College London, London, UK

**ABSTRACT:** The strain field evolution and crack pattern of reinforced concrete attacked by accelerated corrosion have been studied using strain gauges and the digital image correlation (DIC) technique. Results show that there was good consistency between DIC and the classical strain gauges about the strain field evolution of corroding reinforced concrete. Moreover, the strain field and crack behavior of reinforced concrete could be tracked by DIC image pattern intuitively and its stress field could also be calculated by DIC quantitatively. However, the micro-deformation of reinforced concrete could be obtained by DIC because of its test accuracy. When reinforced concrete was attacked by accelerated corrosion, the tension stress was applied to the upper zone of reinforced bar, and the compressive stress was applied to its bottom zone. And the brittle crack was mainly a failure model of reinforced concrete.

**Keyword:** reinforced concrete; accelerated corrosion; DIC; strain field; crack

## **1 INTRODUCTION**

In marine environment, reinforced concrete is widely used as a construction material for infrastructures. But the chloride and sulfate ions in marine environment would penetrate into the concrete cover and induce the depassivation and corrosion of the steel bar [1-2], which could result in corrosive cracking and carrying capacity loss, and ultimately damage the concrete structures [3-4]. Therefore, the corrosion of steel bars induced by salinity is always considered a major threat to the safety of the structures. The deterioration of the steel bars due to corrosion has contributed to more than 80% of all the damages in reinforced concrete structures [5-7]. In severe environments such as marine

tidal zone, corrosion rates even exceed 500  $\mu\text{m}/\text{year}$  [8].

The tensile strength of concrete and expansion stress induced by the corroded reinforced bar are key parameters to the crack time of reinforced concrete and they decide the service life of the concrete structure in a marine environment. Obviously, it is extremely tough to test the expansion stress of the reinforcement corrosion in concrete directly, but the elasticity modulus and deformation evolution induced by reinforcement corrosion could be tested, which is helpful to this issue. Y. Ballim and Goitseone have preliminarily proven the possibility of the considerations above toward midspan and lateral deformation in concrete using strain gauges [9-11]. The classic measurement techniques, such as strain gauges extensometers and linear variable differential transformer sensors (LVDTs), hardly allow for precise estimations of strain fields or for an early crack detection. The strain gauges themselves may break and get destroyed locally at critical sections close to failure. In addition, strain gauges only measure strains at the fixing points and in the direction of the gauges alignment, and therefore, they do not provide a full-field analysis. Digital image correlation (DIC) is a computer vision technique, which has been successfully applied to various mechanical and deformation problems[12-14], owing to its numerous advantages, such as noncontact, full-field measurements, its simplicity in use and the continuous measurements up to failure.

With the aim of continuously monitoring the strain field developments and the cracking process of reinforced concrete under accelerated corrosion, the Digital Image Correlation technique is used. The results of this study are useful for corrosion expansion stress calculation and service life prediction of reinforced concrete in the severe environment.

## 2. EXPERIMENTATION

### 2.1. Materials and specimen preparation

P.I.52.5 Portland cement in accordance with Chinese standard GB175-2007, with a compressive strength of 59.8 MPa at the age of 28 days, was used in this study. Table 1 shows the chemical composition of cement.

**Table 1.** Chemical compositions of Portland cement

Constituent (wt%)	SiO <sub>2</sub>	Al <sub>2</sub> O <sub>3</sub>	Fe <sub>2</sub> O <sub>3</sub>	CaO	MgO	TiO <sub>2</sub>	Na <sub>2</sub> O	K <sub>2</sub> O	SO <sub>3</sub>	Cl
Cement	21.8	5.42	3.44	66.01	1.26	0.36	0.57	0.33	0.66	0.00

The coarse aggregate was crushed granite with a maximum size of 25 mm, and river sand with a fineness modulus of 2.6 was used as the fine aggregate. A polycarboxylic ether-based super plasticizer was used, and its dosage was adjusted to keep the slump of fresh concrete in the range of 140 mm to 180 mm. The concrete mixtures were prepared with an effective water-to-cement ratio (w/c) of 0.33 and 450 kg/m<sup>3</sup> binders. The mixture proportions for the reinforced concrete were 1:1.58:2.37:0.33 for cement: sand: aggregate: water, respectively, and the compressive strengths of the concrete cured for 28 d were 36.5 MPa and 63.9 MPa, respectively.

The size of reinforced concrete specimen was 100×100mm×300mm, and the corrosion solution tank with a size of 15mm\*20\*150mm had reserved on the upper area in the specimens. A carbon steel bar with 10 mm diameter was casted in the middle of the specimen along the length. The carbon steel bar was cleaned and coated with cement paste followed by epoxy coating at the

concrete-air interface. The surface of the deformed carbon steel bar was polished by 200# sand paper. The steel bars were degreased by acetone just before it was placed in the mold. Reinforced concrete samples were cast and placed at room temperature in the mold, which were subsequently removed after 48 h. Finally, all specimens were cured under the condition of  $20^{\circ}\text{C}\pm 3^{\circ}\text{C}$  and 95% relative humidity for 28 d.

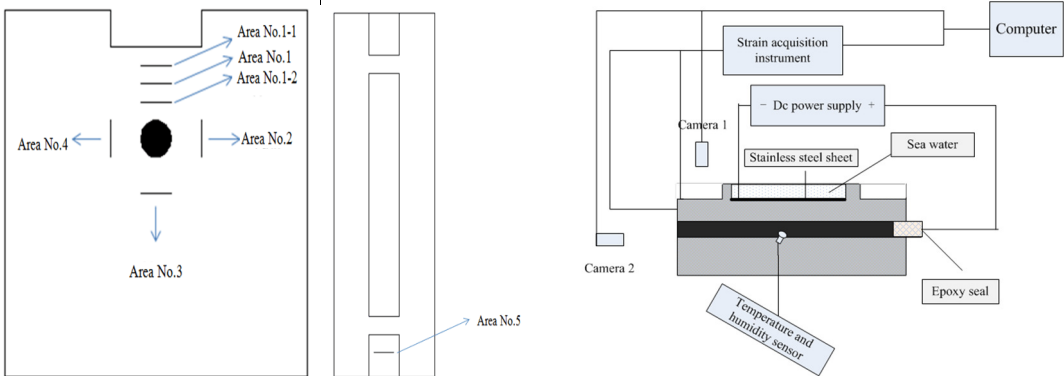
**2.2 Accelerated corrosion of reinforced concrete**

The seawater was poured into the solution tank, and the reinforced concrete was subjected to accelerated corrosion current supplied by a potentiostatic through the carbon steel bar (connected to the positive electrode) and the stainless steel bar (connected to the negative electrode). And the stainless steel bar was placed into the seawater. Further, the electric potential was kept at a constant 30 V, and the current was checked every 1 h.

**2.3 DIC measurement**

The digital images were acquired continuously as the specimen was accelerated corroded. With this technique, the deformation analysis of specimens can be conducted by comparing the deformed images during corrosion with the reference image before corrosion. In deformation identification, a small part of the reference image is defined as the reference subset and the corresponding part on the deformed image as the target subset. The target subset can be searched by gray scale distribution. Thus, deformation measurement is transformed into digital correlation calculation and the displacements at the various points in the reference subset are obtained by subtracting the new coordinates from the original ones.

In the DIC test, two digital cameras with 75 mm macro lens were mounted to capture images of  $100*100\text{ mm}^2$  plate and the upper surface of the specimen. The digital cameras have a resolution of  $1200 * 1600$  pixels and give 256 levels of gray output. The cameras are mounted in order to image an area of  $100 * 100\text{ mm}^2$ . For this resolution, one pixel in the image represents approx.  $80\text{ }\mu\text{m}$  square on the specimen, which is considered sufficient to determine displacement measurement with  $4\text{ }\mu\text{m}$  accuracy. And a uniform/random speckle pattern is applied on the surface of the specimens. In order to compare the strain measurements from conventional measurement devices with those of the DIC system, the conventional measurement devices, the resistance strain gauge were employed to measure the deformation around the reinforced bar. The DIC and strain gauge measurement system are shown in Fig.1.



(a) The analysis area profiles of specimens (b) sketch of DIC

**Fig. 1** The test program of reinforced concrete under accelerated corrosion

### 3 RESULTS AND DISCUSSION

#### 3.1 Electric current

Reinforced concrete specimens were polarized by a constant voltage of 30 V, and the current change with time is shown in Fig. 2. The electric current decreased fast at the early stage, and kept stable to concrete cracks. And then the electric current increased quickly due to the seawater penetration into the surface of reinforced concrete through the crack. With the crack filled with increasing corrosion production, the electric current increased slowly again. When the penetrating crack was shown in the reinforced concrete, the electric current jumped to about 2.5 times of initial value. According to the evolution of electric current, the time of initial crack and penetrating crack was 160h and 256h respectively.

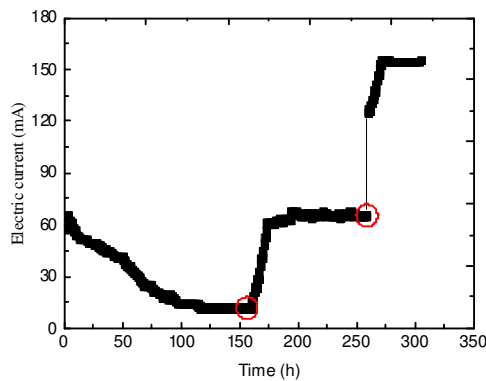


Fig. 2 Electric current evolution of reinforced concrete

#### 3.2 Strain field evolution around reinforced bar

The area around reinforced bar in  $100 \times 100 \text{mm}^2$  plate of reinforced concrete with pixel coordinates  $140 \times 180$  in the image was selected, which is shown in Fig.3. The strain field evolution in these areas was calculated by DIC technique and was plotted in Fig.4. Obviously, the strain field evolution of reinforced concrete under accelerated corrosion can be tested by DIC technique. When reinforced concrete corroded for 256h, the strain around reinforced bar increased about  $8000 \mu\epsilon$ . The strain increased to  $25000 \mu\epsilon$  when the sample corroded for 304h.

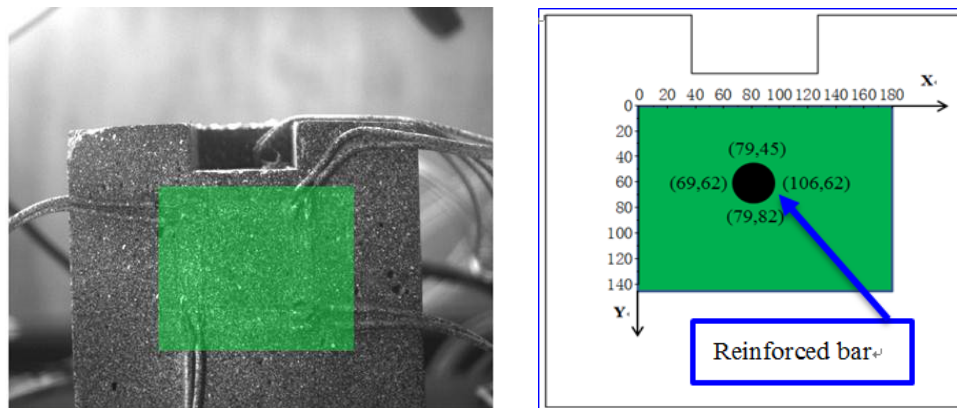
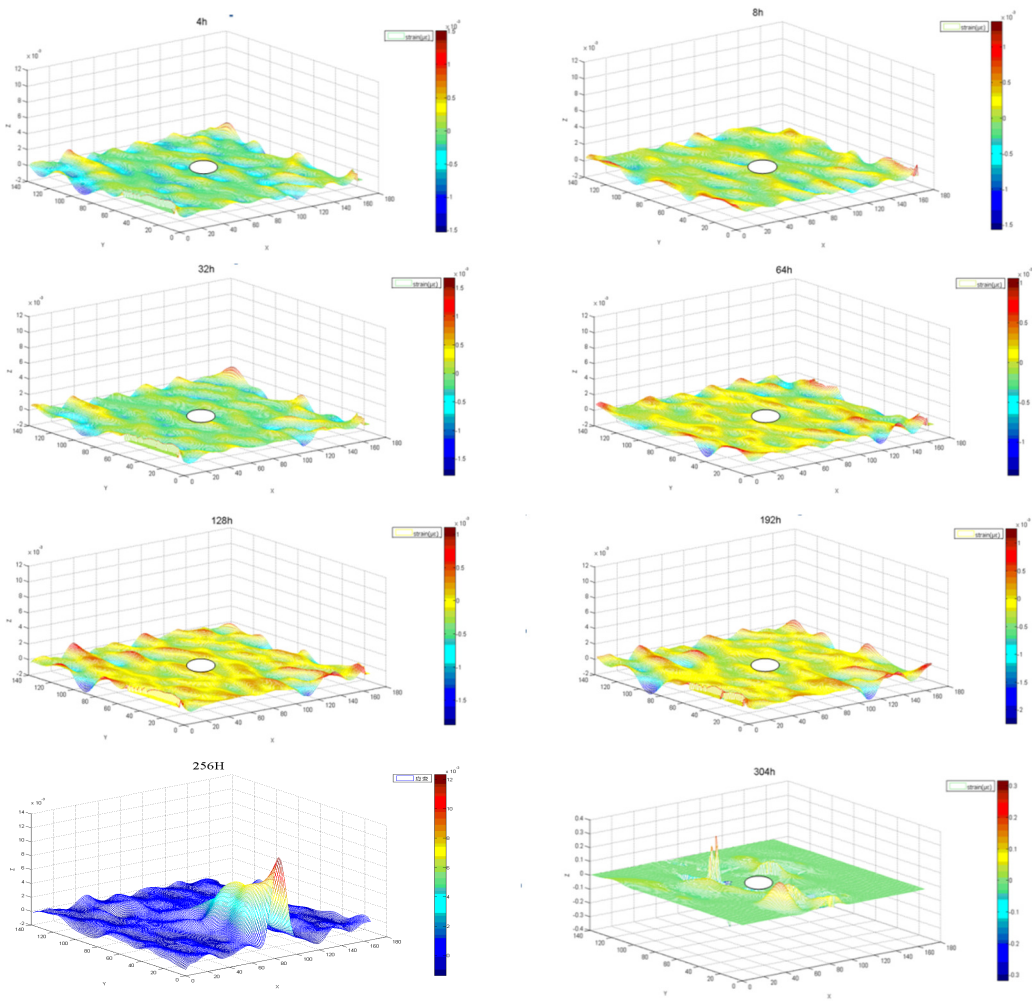
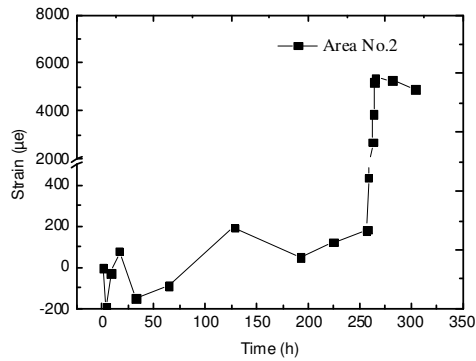
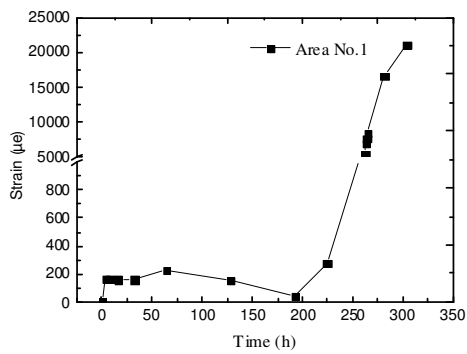


Fig. 3 The location of reinforced bar and strain field analysis area



**Fig. 4** The strain field around reinforced bar in different corrosion time

Based on the strain cloud maps, the strain evolution in location of the strain gauge was calculated and plotted as shown in Fig.5. Obviously, the tension stress induced by the corrosion of reinforced bar was applied to concrete in the upper zone (Area No.1) and the Right zone (Area No.2) of reinforced bar, and compressive stress was applied to concrete in the bottom zone (Area No.2) of reinforced bar. The concrete in the left zone (Area No.3) of reinforced bar bears compressive stress firstly, and then tension stress when penetrating crack occurred in concrete.



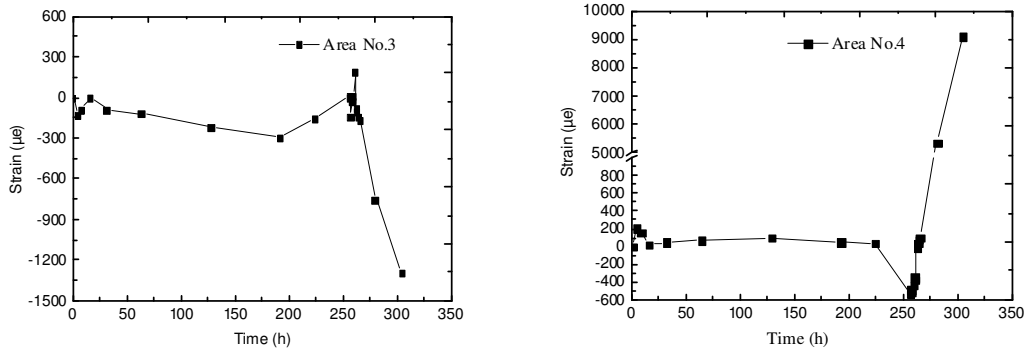


**Fig. 5** Strain evolution in Area1-4 around reinforced bar under accelerated corrosion

The strain measurements obtained by electrical resistance strain gauges around reinforced bar are shown in Fig.6. The rule of strain/stress field evolution around reinforced bar tested by DIC and the strain gauge respectively is consistent. The test accuracy of the strain gauge and DIC was about  $1\ \mu\epsilon$  and  $80\mu\epsilon$  respectively. Therefore, the micro-deformation of concrete could be reflected by the strain gauge, and the crack process of concrete could be tracked by DIC because the strain gauge would be broken when crack occurred on concrete. Fig.7 presents a comparison between the strain measurements obtained by electrical resistance strain gauges and the strains calculated by the DIC technique.

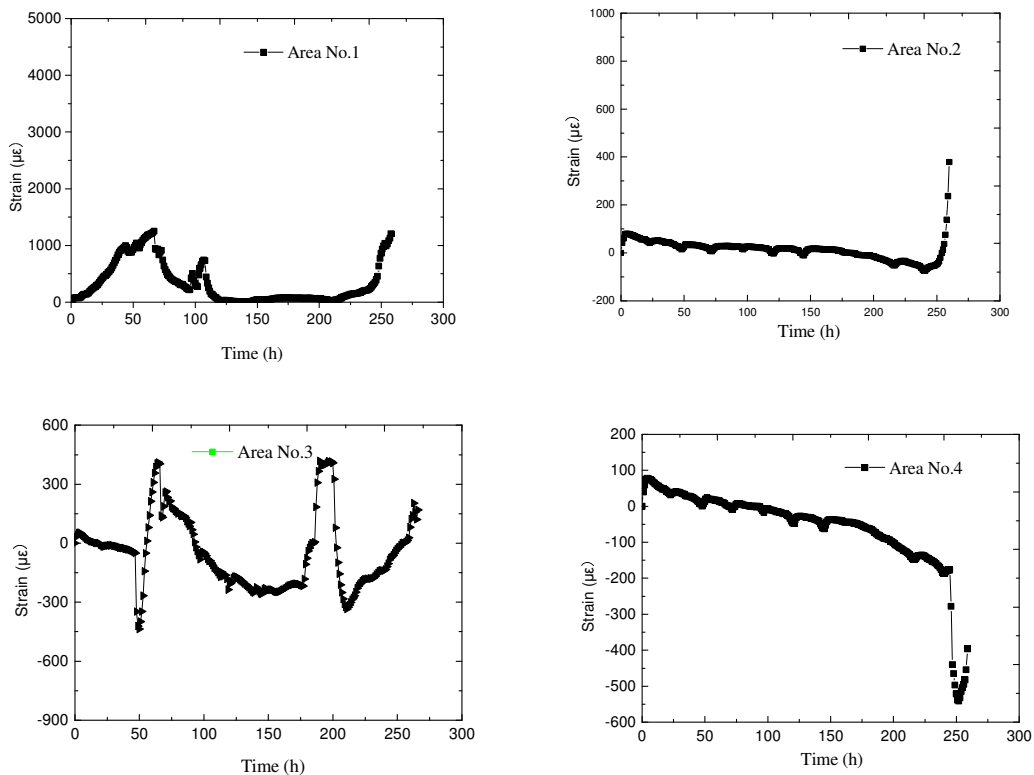
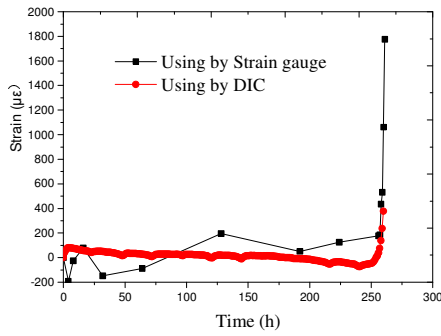
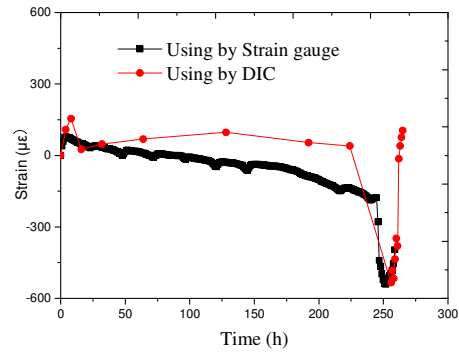


**Fig. 6** the strain field around reinforced bar tested by strain gauge



(a) Area No.2

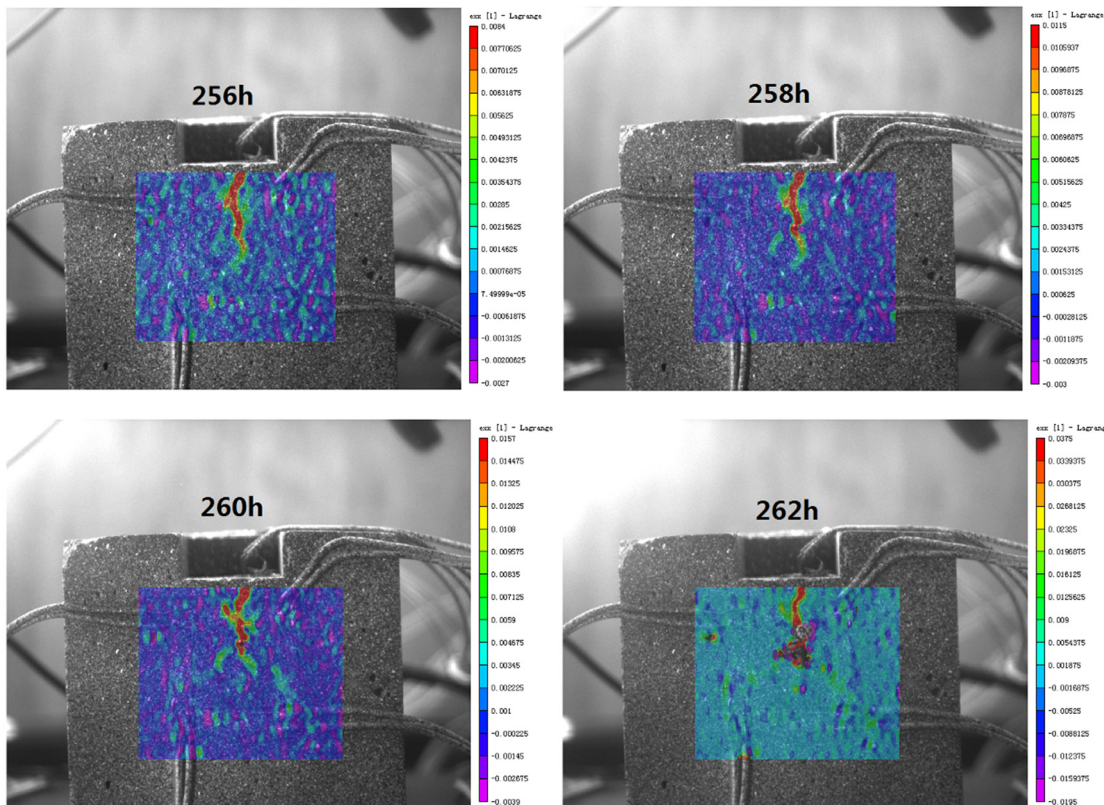


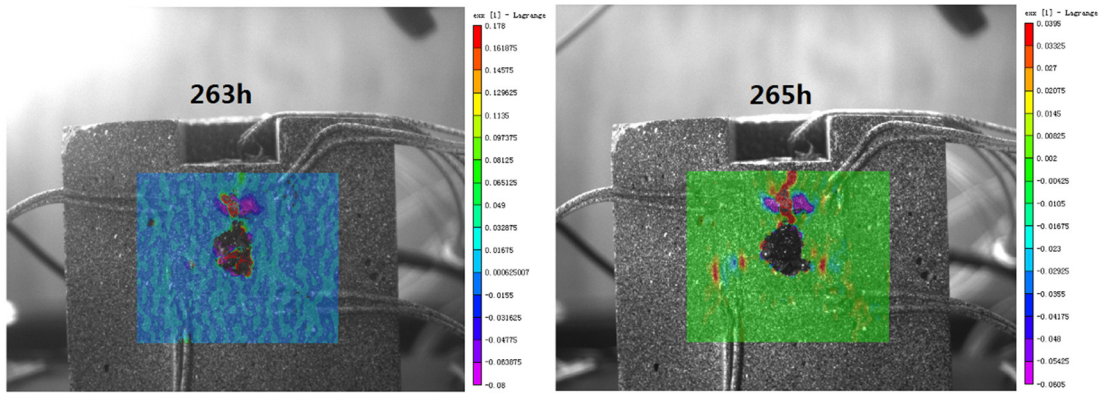
(b) Area No.4

**Fig. 7** Comparison between the strains measurements obtained by strain gauges and DIC

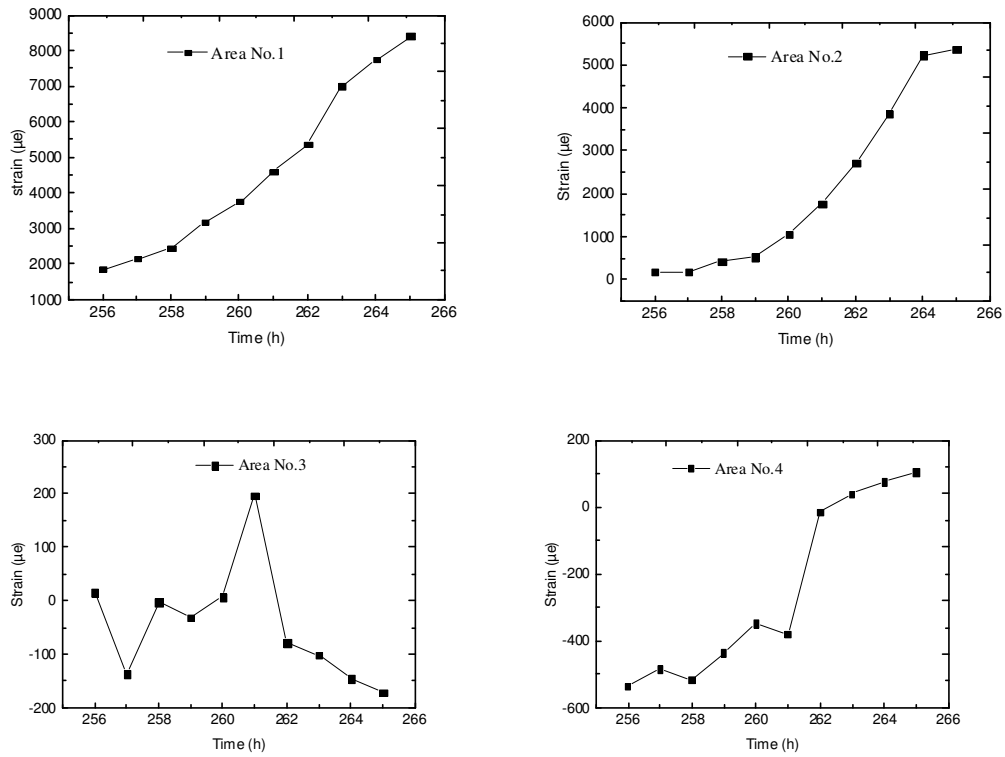
### 3.3 Crack process of concrete tracked by DIC

Fig.8 shows a description of the crack pattern obtained by DIC technique during the accelerated corrosion test. The displacement profile of the DIC qualitatively agrees with the crack pattern observed on the specimens. The brittle crack of concrete under accelerated corrosion could be observed, and the crack width in upper zone of concrete would be kept stable and even be narrowed due to crack occurred on other areas around reinforced bar. According to the DIC profiles, the deformation of concrete around reinforced bar for 10 hours before and after crack was calculated and presented in Fig.9. Additionally, the deformation of concrete from reinforced bar to the upper surface of concrete, and the surface of concrete in Area No.5 was also calculated and shown in Fig.10. Obviously, the crack pattern and deformation could be reflected by DIC technique with image format directly and data format quantitatively.





**Fig. 8** The crack process of concrete induced by corrosion of reinforced bar



**Fig. 9** Deformation of concrete around reinforced bar for 10 hours before and after crack

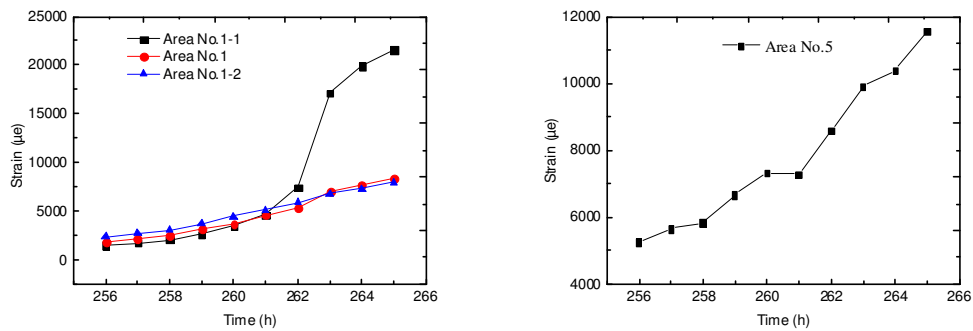


**Fig. 10** Deformation of concrete in the side plate and upper surface



## 4 CONCLUSIONS

The following conclusions can be drawn from the present experimental work using the DIC measurement technique and classical strain gauges:

1. The comparison between the classical measurement techniques such as strain gauges and the DIC technique suggests that the two techniques are suitable for the analysis of strain field of concrete induced by corrosion of reinforced bar. The good agreement about strain and stress field evolution between the two measurement methods indicates that the DIC technique is an efficient measuring tool for obtaining displacement and strain fields during corrosion of reinforced concrete.
2. Measurements of strains and crack process at or after failure of reinforced concrete are possible with DIC technique compared to the classical methods. However, the test accuracy of DIC is lower than that of strain gauges, and it's difficult to track the micro-deformation of reinforced concrete under accelerated corrosion.
3. When reinforced concrete was attacked by accelerated seawater corrosion, the tension stress induced by the corrosion of reinforced bar was applied to concrete in upper zone of reinforced bar and the surface of concrete, and compressive stress was applied to concrete in bottom zone of reinforced bar. The brittle crack failure model occurred on reinforced concrete.

## ACKNOWLEDGMENTS

This work is a part of a series of projects financially supported by the Chinese National Natural Science Foundation (NSF) Grant No. 51378269 and No.51420105015, and the Chinese National 973 project Grant No. 2015CB655100. Besides, this work is also supported by Chinese Railway Foundation Grant No. 2014G004-F. The leading author is sponsored by NSFC for his academic visit at University College London. All these are gratefully appreciated.

## REFERENCES

- [1] T. Cheewaket, C. Jaturapitakkul, W. Chalee. Initial corrosion presented by chloride threshold penetration of concrete up to 10 year-results under marine site. *Construction and Building Materials*, 2012(37) 693-698.
- [2] H. F. Yu, Study on high performance concrete in salt lake: durability, mechanism and service life prediction. Southeast University, Nanjing, 2004.
- [3] Z. Q. Jin, S. Gao, X. Zhao, L. Yang. Corrosive Crack and its 3D Defects Identification of Reinforced Concrete Subjected to Coupled Effect of Chloride Ions and Sulfate Ions. *Int. J. Electrochem. Sci.* 2015(10) 625-636.
- [4] J. Bilcik, I. Holly, Effect of reinforcement corrosion on bond behavior. *Procedia Engineering*, 2013(65) 248-253.
- [5] M.V. Biezma, J.R.San Cristobal. Methodology to study cost of corrosion. *Corrosion Engineering, Science and Technology*, 2005(40) 344-352.
- [6] B.R. Hou, W.H. Li, Z.Q. Jin, et al. Corrosion and repair reinforcement technology of reinforced concrete]. *Science press*, Beijing, 2012.
- [7] M. K. Moradllo, M. Shekarchi, M. Hoseini. Time-dependent performance of concrete

- surface coatings in tidal zone of marine environment. *Construction and Building Materials*, 2012(30)198-205
- [8] A. Costa, J. Appleton. Case studies of concrete deterioration in a marine environment in Portugal. *Cement and Concrete Composites*, 2002(24)169-179.
- [9] Y. Ballim, J.C. Reid., 'Reinforcement corrosion and the deflection of RC beams—an experimental critique of current test methods', *Cement and Concrete Composites*, 25(2003) 625-632.
- [10] Goitseone Malumbela, Pilate Moya, Mark Alexander. Behaviour of RC beams corroded under sustained service loads. *Construction and Building Materials*, 2009(23) 3346-3351.
- [11] Goitseone Malumbela, Mark Alexander, Pilate Moyo. Interaction between corrosion crack width and steel loss in RC beams corroded under load. *Cement and Concrete Research*, 2010(40)1419-1428.
- [12] D.G. Aggelis, S. Verbruggen, E. Tsangouri, T. Tysmans, D. Van Hemelrijck. Characterization of mechanical performance of concrete beams with external reinforcement by acoustic emission and digital image correlation. *Construction and Building Materials*, 2013(47) 1037-1045
- [13] David Corr, Matteo Accardi, Lori Graham-Brady, Surendra Shah. Digital image correlation analysis of interfacial debonding properties and fracture behavior in concrete. *Engineering Fracture Mechanics*, 2007(74) 109-121.
- [14] M. Hamrat, B. Boulekbache, M. Chemrouk, S. Amziane. Flexural cracking behavior of normal strength, high strength and high strength fiber concrete beams, using Digital Image Correlation technique. *Construction and Building Materials*, 2016(106) 678-692.